Two–Loop Bethe Logarithms for non-S Levels

Ulrich D. Jentschura
Max–Planck–Institut für Kernphysik, Saupfercheckweg 1, 69117 Heidelberg, Germany and
National Institute of Standards and Technology, Gaithersburg, Maryland 20899–8401, USA

Two-loop Bethe logarithms are calculated for excited P and D states in hydrogenlike systems, and estimates are presented for all states with higher angular momenta. These results complete our knowledge of the P and D energy levels in hydrogen at the order of $\alpha^8\,m_e\,c^2$, where m_e is the electron mass and c is the speed of light, and scale as Z^6, where Z is the nuclear charge number. Our analytic and numerical calculations are consistent with the complete absence of logarithmic terms of order $(\alpha/\pi)^2\,(Z\alpha)^6\,\ln[(Z\alpha)^{-2}]\,m_e\,c^2$ for D states and all states with higher angular momenta. For higher excited P and D states, a number of poles from lower-lying levels have to subtracted in the numerical evaluation. We find that, surprisingly, the corrections of the "squared decay-rate type" are the numerically dominant contributions in the order $(\alpha/\pi)^2\,(Z\alpha)^6\,m_e\,c^2$ for states with large angular momenta, and provide an estimate of the entire B_{60}-coefficient for Rydberg states with high angular momentum quantum numbers. Our results reach the predictive limits of the quantum electrodynamic theory of the Lamb shift.

PACS numbers: 12.20.Ds, 31.30.Jv, 06.20.Jr, 31.15.-p

I. INTRODUCTION

The two-loop Bethe logarithm stems from a nonrelativistic treatment of the full two-loop self-energy. It is the finite part which is left over when the two-loop problem is renormalized according to the original derivation of Bethe [1] for the one-loop self-energy and therefore represents a natural generalization of the most basic quantum electrodynamic calculation to the two-loop level, yet the respective calculation is the only way to complete the analysis of hydrogenic energy levels in the order $(\alpha/\pi)^2\,(Z\alpha)^6 m_e\,c^2$. In comparison to the one-loop problem, the two-loop nonrelativistic self-energy is much more complicated, and it involves three instead of one propagator denominators. Matrix elements cannot be expressed in closed analytic form. Numerical methods, inspired by lattice calculations, represent convenient tools for the evaluations.

Final calculations were carried out on workstation clusters of the Max–Planck–Institute for Nuclear Physics in Heidelberg and of the National Institute of Standards and Technology. The total CPU time of all computations required for the present paper was about 30 months, but the real time was of course drastically shortened due to parallel processing. The two-loop problem is known to be computationally demanding. Additional difficulties arise for excited states due to a number of poles from lower-lying levels which have to be subtracted in the numerical evaluation. After subtraction, the result is finite, as it should be, and represents an observable energy shift.

The problem of so-called squared decay rates is associated with the two-loop Bethe logarithm [2]. The squared decay rates, which originate from specific photon energies where two propagators become singular simultaneously, cannot be uniquely interpreted as energy corrections even if the concept of a pole on the second sheet of the Riemann surface defining the propagator is used in order to define energy levels, and have been assigned [2] to an contribution δB_{60}, where B_{60} is the two-loop coefficient multiplying the scaling factor of $(\alpha/\pi)^2\,(Z\alpha)^6 m_e c^2/n^3$ (here, n is the principal quantum number). For $3P$ and $4P$ states, the squared decay rates were originally evaluated in in Ref. [2]. In [3], an analysis of S states was supplemented, and it has been clarified that the contributions as given in [2] should be understood in radians per second rather than cycles per second, or Hz. Here, we supply numerical values for the correction of the "squared-decay" type for excited S, P, D, F, G and H states, and we also discuss approximations for general states. The squared decay rates are a manifestation of the fact that a proper definition of energy levels ceases to be possible at the level of $\alpha^2(Z\alpha)^6$ in units of the electron mass, as already pointed out in Ref. [4]. Yet, these contributions are mathematically well defined and have to be evaluated in a calculation whose aim is to explore the predictive limits of the quantum electrodynamic theory of hydrogenlike systems.

This paper is organized as follows. In Sec. II, we summarize all known results for the two-loop energy shift of excited P and D states up to the order $\alpha\,(Z\alpha)^6$ (all energy shifts are measured in units of $m_e\,c^2$ in this paper unless stated otherwise). Important definitions and formulas regarding the two-loop Bethe logarithm are recalled in Sec. III. The asymptotics of the two-loop integrand and the calculation of the two-loop Bethe logarithm are discussed in Sec. IV. The squared decay rates, which are numerically significant especially for states with higher angular momenta, are treated in Sec. V. Miscellaneous two-loop results are compiled in Appendixes A—C. One-photon vacuum-polarization and self-energy shifts of order $\alpha(Z\alpha)^7$ are discussed in Appendix D.

II. KNOWN TWO–LOOP RESULTS

We work in natural units ($\hbar = c = \epsilon_0 = 1$), as is customary in QED bound-state calculations, and we also set the electron mass equal to unity in the following. The real part of the energy displacement of a hydrogenic state due to the two-loop (2L) self-energy (SE) can be parameterized as follows,

$$\Delta E^{(2L)}_{SE} = \left(\frac{\alpha}{\pi}\right)^2 \frac{(Z\alpha)^4}{n^3}\,H(Z\alpha)\,, \qquad (1)$$

where H is a dimensionless function. Here, we are concerned with P and D states, and in part with states of higher angular momenta. For these manifolds, the first nonvanishing terms in the semi-analytic expansion of the dimensionless function $H(Z\alpha)$ in powers for $Z\alpha$ and $\ln(Z\alpha)$ read as follows,

$$H(Z\alpha) \;=\; B_{40} + (Z\alpha)^2 \Big\{ B_{62}\ln^2[(Z\alpha)^{-2}] + B_{61}\ln[(Z\alpha)^{-2}] + B_{60} \Big\}. \tag{2}$$

The first index of the B-coefficients denotes the power of $Z\alpha$ including the factors $Z\alpha$ contained in Eq. (1), and the second index denotes the power of $\ln[(Z\alpha)^{-2}]$. For the lowest-order B_{40} term, a complete result is known which is valid for any hydrogenic state (see, e.g., Ref. [5]). We here express the result in terms of the expectation value of an operator, as in Eq. (8.1) of Ref. [6], and suppress all operators which are zero for P states and states with higher angular momenta,

$$\frac{(Z\alpha)^4}{n^3}\,B_{40} \;=\; \left[\frac{197}{288} - \frac{3}{2}\,\zeta(2)\,\ln 2 + \frac{1}{4}\,\zeta(2) + \frac{3}{8}\,\zeta(3)\right] \times \left\langle \sigma^{ij}\,\nabla^i V\,p^j \right\rangle .$$

We adopt here all conventions of Ref. [6], in particular $\sigma^{ij} = [\sigma^i,\,\sigma^j]/(2\,\mathrm{i})$ for the (2×2)-dimensional spin matrices. We recall the well-known identity

$$\left\langle \sigma^{ij}\,\nabla^i V\,p^j \right\rangle = \frac{(Z\alpha)^4}{n^3}\,\left(-\frac{2}{\kappa\,(2l+1)}\right), \tag{3}$$

where $\kappa = (-1)^{j+l+1/2}\,\left(j+\frac{1}{2}\right)$ is the Dirac angular quantum number (l is the orbital angular momentum quantum number, and j denotes the total angular momentum of the electron). In this way, one immediately reproduces the well-known general result

$$B_{40} \;=\; -\frac{2}{\kappa\,(2l+1)} \times \left[\frac{197}{288} - \frac{3}{2}\,\zeta(2)\,\ln 2 + \frac{1}{4}\,\zeta(2) + \frac{3}{8}\,\zeta(3)\right], \tag{4}$$

which is valid for all non-S hydrogenic states.

Our goal here is to extend formula (4) to two relative orders of $Z\alpha$, for general P and D states, and to find estimates for general states with higher angular momenta. In Ref. [6], numerical results have only been indicated for the fine-structure difference of D states [see Eqs. (4.22) and (5.3) of Ref. [6]] and for P states [see Eqs. (4.24) and (5.4), (6.2) and (7.7) of Ref. [6]]. However, the complete result for B_{60} entails the two-loop Bethe logarithm, which has not been known so far.

We recall that in terms of matrix elements, to be evaluated on Pauli–Schrödinger nonrelativistic wave functions of non-S hydrogenic states, the higher-order terms B_{62}, B_{61} and B_{60} can be expressed as follows (see Ref. [6]),

$$\begin{aligned}
\frac{(Z\alpha)^6}{n^3}\left\{B_{62}\ln^2[(Z\alpha)^{-2}] + B_{61}\ln[(Z\alpha)^{-2}] + B_{60}\right\} &= \frac{(Z\alpha)^6}{n^3}\left\{b_L + \beta_4 + \beta_5 + \left[\frac{38}{45} + \frac{4}{3}\ln\left[\tfrac{1}{2}(Z\alpha)^{-2}\right]\right] N\right\} \\
&+ \left[-\frac{42923}{259200} + \frac{9}{16}\zeta(2)\ln(2) - \frac{5\zeta(2)}{36} - \frac{9\zeta(3)}{64} + \frac{19}{135}\ln\left[\tfrac{1}{2}(Z\alpha)^{-2}\right] + \frac{1}{9}\ln^2\left[\tfrac{1}{2}(Z\alpha)^{-2}\right]\right]\left\langle \vec\nabla^2 V \frac{1}{(E-H)'}\vec\nabla^2 V\right\rangle \\
&+ \left[\frac{2179}{10368} - \frac{9}{16}\,\zeta(2)\,\ln(2) + \frac{5}{36}\,\zeta(2) + \frac{9}{64}\,\zeta(3)\right]\left\langle \vec\nabla^2 V\,\frac{1}{(E-H)'}\,\vec p^{\,4}\right\rangle \\
&+ \left[-\frac{197}{1152} + \frac{3}{8}\,\zeta(2)\,\ln(2) - \frac{1}{16}\,\zeta(2) - \frac{3}{32}\,\zeta(3)\right]\left\langle \vec p^{\,4}\,\frac{1}{(E-H)'}\,\sigma^{ij}\,\nabla^i V\,p^j\right\rangle \\
&+ \left[\frac{233}{576} - \frac{3}{4}\,\zeta(2)\,\ln(2) + \frac{1}{8}\,\zeta(2) + \frac{3}{16}\,\zeta(3)\right]\left\langle \sigma^{ij}\,\nabla^i V\,p^j\,\frac{1}{(E-H)'}\,\sigma^{ij}\,\nabla^i V\,p^j\right\rangle \\
&+ \left[-\frac{197}{2304} + \frac{3}{16}\,\zeta(2)\,\ln(2) - \frac{1}{32}\,\zeta(2) - \frac{3}{64}\,\zeta(3)\right]\left\langle \left\{\vec p^{\,2}, \vec\nabla^2 V + 2\,\sigma^{ij}\,\nabla^i V\,p^j\right\}\right\rangle \\
&+ \left[-\frac{83}{1152} + \frac{17}{8}\zeta(2)\ln(2) - \frac{59}{72}\,\zeta(2) - \frac{17}{32}\,\zeta(3)\right]\left\langle \left(\vec\nabla V\right)^2\right\rangle \\
&+ \left[-\frac{87697}{345600} + \frac{9}{10}\zeta(2)\,\ln(2) - \frac{2167}{9600}\zeta(2) - \frac{9}{40}\zeta(3) + \frac{19}{270}\ln\left[\tfrac{1}{2}(Z\alpha)^{-2}\right] + \frac{1}{18}\ln^2\left[\tfrac{1}{2}(Z\alpha)^{-2}\right]\right]\left\langle \vec\nabla^4 V\right\rangle \\
&+ \left[-\frac{16841}{207360} - \frac{1}{5}\,\zeta(2)\,\ln(2) + \frac{223}{2880}\,\zeta(2) + \frac{1}{20}\,\zeta(3) + \frac{1}{24}\ln\left[\tfrac{1}{2}(Z\alpha)^{-2}\right]\right]\left\langle 2\,\mathrm{i}\,\sigma^{ij}\,p^i\,\vec\nabla^2 V\,p^j\right\rangle .
\end{aligned} \tag{5}$$

We take the opportunity to point out that in the corresponding Eq. (8.1) of Ref. [6], a prefactor of $(\alpha/\pi)^2$ in front of the second term on the right-hand side was missing [in Ref. [6], the entire above result (5) for the energy shift was multiplied by a factor of $(\alpha/\pi)^2$ on the left and right-hand side]. Also, the square of the logarithm $\ln^2\left[\frac{1}{2}(Z\alpha)^{-2}\right]$ in the second and in the last-but-one term on the right-hand side were not included. Both typographical errors are absent from Eq. (8) of previous work reported in Ref. [7] and from the above Eq. (5).

We recall here the definitions of the quantities N, β_4 and β_5, which enter into Eq. (5). In doing so, we first recall that in accordance with the notation introduced in [7], we redefine the finite part of an integral which diverges as

$$\int_0^\Lambda dk\, f(k) = A\,\lambda + B\,\ln\lambda + C + \mathcal{O}(\lambda^{-1})\,, \qquad (6a)$$

with $\lambda \equiv \Lambda\,(Z\,\alpha)^{-2}$, for a specified upper cutoff Λ, to be equal to just the constant term, i.e.

$$\int_0^\Lambda dk\, f(k) \equiv C. \qquad (6b)$$

With this definition in mind, we have

$$\begin{aligned}
\frac{(Z\alpha)^6\,N}{n^3} &= \frac{2}{3} Z\,\alpha \int_0^\Lambda dk k\,\delta_{\pi\,\delta^3(r)} \left\langle \vec{p}\,\frac{1}{E-H-k}\,\vec{p}\right\rangle,\\
\frac{(Z\alpha)^6\,\beta_4}{n^3} &= \frac{2}{3}\int_0^\Lambda dk k \delta_{(\sigma^{ij}\nabla^i\,V\,p^j/4)} \left\langle \vec{p}\frac{1}{E-H-k}\vec{p}\right\rangle,\\
\frac{(Z\alpha)^6\,\beta_5}{n^3} &= -\frac{1}{2}\int_0^\Lambda dk k \left\langle \sigma^{ij}\nabla^j V\frac{1}{E-H-k}p^i\right\rangle. \qquad (7)
\end{aligned}$$

The N term has previously been defined in Refs. [8, 9]; it is generated by a Dirac delta correction to the Bethe logarithm. The notation δ_V is used in accordance with Ref. [6, 8] in order to denote the first-order perturbation of the Hamiltonian, the energy and the wave function in the ensuing matrix element, due to the specified potential V.

The evaluation of the two-loop Bethe logarithm for $1S$ and $2S$ has been discussed in Ref. [9], and for $3S$–$6S$ in Ref. [3]. For $1S$ and $2S$, there is no ambiguity in the definition of the Bethe logarithm, because the integration over both photon energies in the nonrelativistic self-energy is free of singularities. However, for all higher excited S states and all states considered here, one incurs real (rather than imaginary) contributions to the energy shift from the product of imaginary contributions due to singularities along both photon integrations, and these result in "squared decay rates" in the sense of Ref. [2]. Thus, it is helpful to make a clear distinction between the singularity-free, principal-value part $\overline{b}_L$ and a real part $\delta^2 B_{60}$, which is incurred by "squared" (or, more precisely, products of) imaginary contributions from the pole terms. We write

$$b_L = \overline{b}_L + \delta^2 B_{60}\,, \qquad (8)$$

where $\overline{b}_L$ is obtained as the nonlogarithmic energy shift stemming from the nonrelativistic self-energy, with all integrations carried out by principal value, and $\delta^2 B_{60}$ is the corresponding contribution defined in Refs. [2, 3], due to squared imaginary parts. The exact meaning of the separation (8) will be clarified below. Here, we just note that for $3S$–$6S$ states, the above separation is not really essential, because $\delta^2 B_{60}$ is a numerically marginal contribution as compared to $\overline{b}_L$ (see Ref. [3]), and thus $b_L(nS) \approx \overline{b}_L(nS)$ to a very good approximation. For the states under investigation here, the distinction (8), surprisingly, proves to be highly essential; yet before we come to a discussion of this surprising phenomenon, let us first discuss the evaluation of $\overline{b}_L$.

III. TWO–LOOP BETHE LOGARITHM

We briefly recall [3, 9] the nonrelativistic two-photon self-energy $\Delta E_{\rm NRQED}$ as an integral of the following structure,

$$\Delta E_{\rm NRQED} = \left(\frac{2\alpha}{3\pi m^2}\right)^2 \int_0^{\epsilon_1} dk_1\, k_1 \int_0^{\epsilon_2} dk_2\, k_2\, f(k_1,k_2)\,, \qquad (9)$$

where the k_1 and k_2 represent photon energies, and ϵ_1 as well as ϵ_2 are cutoff parameters. The function $f(k_1,k_2)$ is defined in Eq. (11) below; its precise structure is unimportant for the following consideration, which concerns the relation of the cutoff parameters ϵ_i ($i=1,2$) to the ultraviolet cutoff Λ parameter used in Eqs. (6)—(7).

In order to clarify this relation, we recall that in the context of the ϵ method (see §123 of Ref. [10] and [11–13]), the cutoff parameters are chosen so that the ϵ can be made arbitrarily small, but only under the condition $Z\alpha \ll \epsilon$, so that the expansion, first carried out in $Z\alpha$, then in ϵ, for the low- as well as the high-energy parts, gives the complete result for the self-energy. This procedure has been fully clarified in §123 of Ref. [10] and in Refs. [11–14]. In Ref. [14], it has been stressed that this method actually corresponds to an expansion in *large* ϵ, and indeed, in the context of the dimensional regularization method [6], the nonlogarithmic term which remains after subtraction of the divergent contributions as $\epsilon_1 = \Lambda_1 \to \infty$, $\epsilon_2 = \Lambda_2 \to \infty$, has been been identified as the two-loop Bethe logarithm b_L. Because we are dealing here with excited states that can decay via dipole radiation, care must be taken in the definition of the integration prescription for the k_1 and k_2 integrations. In the current section, we first assume a principal-value prescription and write

$$\begin{aligned}
&\frac{(Z\alpha)^6}{n^3}\,\overline{b}_L = \qquad (10)\\
&\qquad \frac{4}{9}(\mathrm{P.V.})\int_0^{\Lambda_1} \mathrm{d}k_1 k_1 (\mathrm{P.V.})\int_0^{\Lambda_2} \mathrm{d}k_2 k_2 f(k_1,k_2),
\end{aligned}$$

where $(\mathrm{P.V.})$ denotes the principal value, and it is understood that divergent terms for large Λ_1 and Λ_2 have to be subtracted, in the sense of Eq. (6).

The subtractions for large Λ_i ($i=1,2$) are carried out assuming $\Lambda_1 \ll \Lambda_2$, so we first let $\Lambda_2 \to \infty$, extract the constant term as a function of k_1 and then we integrate this term with respect to k_1, letting $\Lambda_1 \to \infty$. In this way we "sweep"

the entire first quadrant of the two-dimensional (k_1, k_2) plane (i.e., the entire region $k_1 > 0$, $k_2 > 0$). Of course, the same result would be obtained for the constant term under the opposite sequence of first letting Λ_1 approach infinity, then Λ_2.

We are now in the position to recall the explicit form of $f(k_1, k_2)$, which reads

$$
\begin{aligned}
f(k_1,k_2) = &- \left\langle p^i \, \frac{1}{H-E+k_1} \, p^j \, \frac{1}{H-E+k_1+k_2} \, p^i \, \frac{1}{H-E+k_2} \, p^j \right\rangle \\
&- \frac{1}{2} \left\langle p^i \frac{1}{H-E+k_1} p^j \frac{1}{H-E+k_1+k_2} p^j \frac{1}{H-E+k_1} p^i \right\rangle - \frac{1}{2} \left\langle p^i \frac{1}{H-E+k_2} p^j \frac{1}{H-E+k_1+k_2} p^j \frac{1}{H-E+k_2} p^i \right\rangle \\
&- \left\langle p^i \frac{1}{H-E+k_1} p^i \left(\frac{1}{H-E} \right)' p^j \frac{1}{H-E+k_2} p^j \right\rangle + \frac{1}{2} \left\langle p^i \, \frac{1}{H-E+k_1} \, p^i \right\rangle \left\langle p^j \left(\frac{1}{H-E+k_2} \right)^2 p^j \right\rangle \\
&+ \frac{1}{2} \left\langle p^i \, \frac{1}{H-E+k_2} \, p^i \right\rangle \left\langle p^j \left(\frac{1}{H-E+k_1} \right)^2 p^j \right\rangle + \left\langle p^i \, \frac{1}{H-E+k_1} \, \frac{1}{H-E+k_2} \, p^i \right\rangle \\
&+ \frac{1}{k_1+k_2} \left\langle p^i \, \frac{1}{H-E+k_2} \, p^i \right\rangle + \frac{1}{k_1+k_2} \left\langle p^i \, \frac{1}{H-E+k_1} \, p^i \right\rangle . \qquad (11)
\end{aligned}
$$

The interpretation of the terms on the right-hand side is as follows: the first six are due to fourth-order perturbation theory generated by the "velocity-gauge" nonrelativistic $(\vec{p}\cdot\vec{A})$-interaction. Herein, the fifth and the sixth terms are derivative terms which naturally occur in fourth-order perturbation theory. The seventh term involves (on the left and on the right) $(\vec{p}\cdot\vec{A})$-interactions, and a seagull term proportional to $\vec{A}^2$ in between. The eighth and ninth terms involve a seagull term outside of the $(\vec{p}\cdot\vec{A})$-interactions. We also recall that the scaling of $f(k_1, k_2)$ with $Z\alpha$ is completely clarified in Ref. [3].

IV. ASYMPTOTICS OF THE INTEGRAND

We first consider the asymptotics relevant for the initial k_2 integration in Eq. (10). In the limit $k_2 \gg k_1$, we find

$$
\begin{aligned}
k_2 \, f(k_1,k_2) &= \left\langle p^i \, \frac{H-E}{(H-E-k_1)^2} \, p^i \right\rangle \qquad (12) \\
&+ \frac{1}{k_2} \, (Z\,\alpha) \, \delta_{\pi\delta^3(r)} \left\langle p^i \, \frac{1}{E-H-k_1} \, p^i \right\rangle + \mathcal{O}\left(\frac{1}{k_2^2}\right) .
\end{aligned}
$$

The second term vanishes for D states and all states with higher angular momenta. Subtracting the two above terms according to the definition (6) [a practical procedure is outlined in Eq. (26) of Ref. [3]], we obtain

$$
g(k_1) = (\mathrm{P.V.}) \int_0^{\Lambda_2} dk_2 \, k_2 \, f(k_1,k_2) \, . \qquad (13)
$$

We now have to calculate

$$
\frac{(Z\alpha)^6}{n^3} \, \overline{b}_L = \frac{4}{9} (\mathrm{P.V.}) \int_0^{\Lambda_1} dk_1 \, k_1 \, g(k_1) \, , \qquad (14)
$$

and this necessitates the calculation of the asymptotics of $g(k_1)$ for large k_1. After a rather long and tedious calculation, we find

$$
k_1 \, g(k_1) = -2 \, \ln k_0 + \frac{3N}{2k_1} + \mathcal{O}\left(\frac{1}{k_1^2}\right) , \qquad (15)
$$

a result which is valid only for non-S states. The N term, which is defined in Eq. (7), remains important for the P state calculation, but vanishes for D states and all states of higher angular momenta.

In the actual calculations, we use a lattice formulation of the Schrödinger propagator [15] with up to 200 000 lattice sites. This provides sufficient accuracy (and computational efficiency) for all calculations reported here and is feasible on average-size workstation clusters.

It is computationally advantageous to isolate the contribution to $\overline{b}_L$ due to the fourth term on the right-hand side of Eq. (8), in order to avoid numerical problems associated with the calculation of the reduced Green function. This contribution reads, after the k_1 and k_2-integrations and appropriate subtractions,

$$
\begin{aligned}
\frac{(Z\alpha)^6}{n^3} \, L_2 = &\frac{4}{9} \sum_{\phi_m \neq \phi} \frac{1}{E-E_m} \\
&\times \left| \left\langle \phi \left| p^i (H-E) \ln \left[\frac{|H-E|}{(Z\alpha)^2} \right] p^i \right| \phi_m \right\rangle \right|^2 , \qquad (16)
\end{aligned}
$$

where ϕ is the reference state. The calculation of this contribution is done separately, by writing it in terms of a sum over virtual states, which are calculated as a basis set on a lattice in coordinate space. Numerical values are compiled in Table I, where the name "loop-after-loop" should be taken *cum grano*

salis because the negative-energy virtual states are excluded from expression (16). The final results for $\overline{b}_L$ are in Table II.

Based on the trend of the data in Table II, we conjecture here that in the limit $n \to \infty$, the two-loop Bethe logarithms for a given l should approach a constant in the same way as the one-loop Bethe logarithms [16–18]. Also, the data in Table II indicate that the two-loop Bethe logarithms, just like their one-loop counterparts, become smaller in magnitude for increasing orbital angular momentum. Indeed, they do so quite drastically, with the D-state values being almost two orders of magnitude smaller than the P-state logarithms. The magnitude of the S-state logarithms [3], in turn, is in the range of $60 \ldots 80$ and thus larger than the P-state values by more than one order of magnitude.

V. SQUARED DECAY RATES

As clarified in Ref. [2] and Sec. IV of Ref. [3], squared decay rates represent natural limits to which energy levels can be uniquely associated with a particular atomic level. Corrections of this type have been analyzed for $2P$ and $3P$ in Ref. [2], and for $3S$ and $4S$ in Ref. [3]. Here, we supplement values for $5P$ and $6P$, as well as all other states with $n \leq 6$. Some inaccuracies in previous treatments for S and P states are corrected in Table III, and a more extensive list of levels is covered.

TABLE I: Loop-after-loop contribution L_2 to the two-loop Bethe logarithm for P, D and F states. For the $6H$ state, the result for the loop-after-loop contribution reads $-0.000(1)$, implying a negative sign.

level	L_2	level	L_2	level	L_2	level	L_2	level	L_2
$2P$	$-0.97(2)$	–	–	–	–	–	–	–	–
$3P$	$-1.15(2)$	$3D$	$-0.004(1)$	–	–	–	–	–	–
$4P$	$-1.19(2)$	$4D$	$-0.004(1)$	$4F$	$-0.002(1)$	–	–	–	–
$5P$	$-1.23(2)$	$5D$	$-0.005(1)$	$5F$	$-0.002(1)$	$5G$	$-0.001(1)$	–	–
$6P$	$-1.26(3)$	$6D$	$-0.005(1)$	$6F$	$-0.002(1)$	$6G$	$-0.001(1)$	$6H$	$-0.000(1)$

According to Refs. [2, 3], the term $\delta^2 B_{60}$ is generated by "squared decay rates," which correspond to well-defined, isolated points of the (k_1, k_2)-photon energy plane, where two propagators become singular simultaneously in the integrand of the two-loop Bethe logarithm given in Eq. (11). These are all points where, for a given principal quantum number n of the reference state, any two of the following conditions are satisfied simultaneously,

$$k_1 = -(Z\alpha)^2 \left(\frac{1}{2n^2} - \frac{1}{2m_1^2}\right), \tag{17}$$

$$k_2 = -(Z\alpha)^2 \left(\frac{1}{2n^2} - \frac{1}{2m_2^2}\right), \tag{18}$$

$$k_1 + k_2 = -(Z\alpha)^2 \left(\frac{1}{2n^2} - \frac{1}{2m^2}\right), \tag{19}$$

where $m_1, m_2, m < n$ are values of the principal quantum numbers in the intermediate states. In Fig. 1, we list all of these points in the two-dimensional (k_1, k_2)-plane for a state with a principal quantum number $n = 6$. All frequencies which give rise to the singularities are smaller than $(Z\alpha)^2/2 = Z^2 R_\infty$.

Upon picking up the squared imaginary contribution, we obtain for the following structures from the two-loop integrand (11),

$$\int_0^{\Lambda_1} dk_1 \int_0^{\Lambda_2} dk_2 \frac{1}{k_1 - a} \frac{1}{(k_2 - b)^2} \to 0\,, \tag{20a}$$

$$\int_0^{\Lambda_1} dk_1 \int_0^{\Lambda_2} dk_2 \frac{1}{(k_1 - a)^2} \frac{1}{k_2 - b} \to 0\,, \tag{20b}$$

$$\int_0^{\Lambda_1} dk_1 \int_0^{\Lambda_2} dk_2 \frac{1}{k_1 - a} \frac{1}{k_2 - b} \to -\pi^2\,, \tag{20c}$$

$$\int_0^{\Lambda_1} dk_1 \int_0^{\Lambda_2} dk_2 \frac{1}{k_1 - a} \frac{1}{k_1 + k_2 - b} \to -\pi^2\,. \tag{20d}$$

One might ask why the result on the right-hand side reads $-\pi^2$, not $-(2\pi)^2$. The answer is that both the k_1 and the k_2 integration contours have to be deformed along *half* circles, centered at the location of the singularities, infinitesimally below the real axis, i.e. in the mathematically positive sense. This half circle entails a factor $\pi\mathrm{i}$, whose square gives the results on the right-hand sides of Eqs. (20a)—(20d).

Finally, the total squared decay rate

$$\delta^2\Gamma = \left(\frac{\alpha}{\pi}\right)^2 \frac{(Z\alpha)^2}{n^3}\, \delta^2 B_{60} \tag{21}$$

is obtained after picking up all terms which result as the product of two imaginary parts, when integrating over both k_1 and

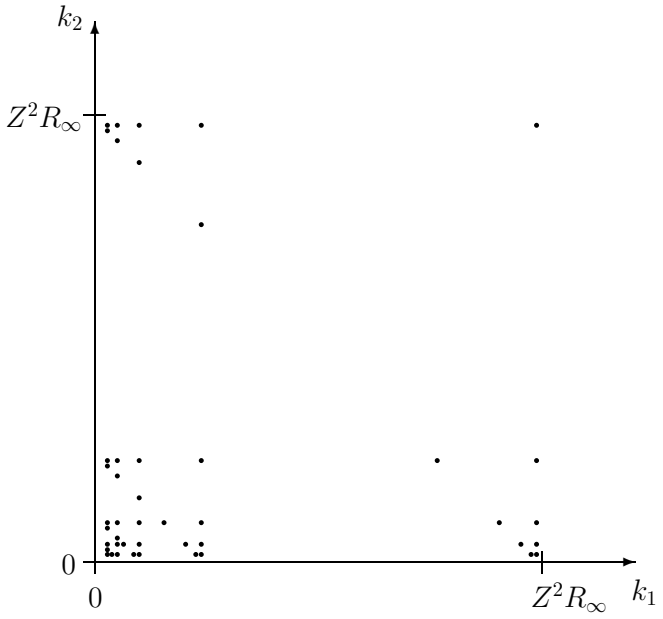

FIG. 1: Location of the discrete pairs of frequencies (k_1, k_2) which give rise to the squared decay rates for an $n = 6$ state. The point $Z^2R_\infty = (Z\alpha)^2 m/2$ denotes a "Z-dependent Rydberg constant" and marks the ionization energy of a nonrelativistic hydrogenlike atom system.

k_2 in Eq. (11), according to the prescription (20). The contributions $\delta^2 B_{60}$ is thus mathematically well-defined and, in particular, has an unambiguously defined sign for each individual state.

A very curious observation can be made regarding the order-of-magnitude of b_L versus that of $\delta^2 B_{60}$ for different manifolds of hydrogenic states. For S and P states, we have $|\delta^2 B_{60}| \ll |b_L|$, as is evident from Table II of this work and from Table II of Ref. [3]. For the $1S$ and the $2S$ states considered in Ref. [9], we even have $\delta^2 B_{60}(1S) = \delta^2 B_{60}(2S) = 0$. For higher excited S states, the magnitude of $\delta^2 B_{60}$ is smaller than the magnitude of the current numerical uncertainty of $\overline{b}_L$ incurred by the numerical integration described in Ref. [3], and thus, $\delta^2 B_{60}$ can at present be completely ignored for S states. Therefore, the question of whether to include $\delta^2 B_{60}$ into the canonical definition of b_L had been ignored in Refs. [3, 9] for the simple reasons that $\delta^2 B_{60}(nS)$ was either vanishing or found to be a numerically negligible. Initially (see Ref. [2]), the notation $\delta^2 B_{60}$ was chosen such as to make an association with a small "uncertainty" in the definition of b_L. However, the situation changes drastically for P states, where $|\delta^2 B_{60}| \approx 0.1\,|b_L|$ for $n \geq 3$, and even more drastically for D states, where $|\delta^2 B_{60}| \gg |b_L|$ for all n, reversing the hierarchy of the "uncertainty" $\delta^2 B_{60}$ and the two-loop Bethe logarithm b_L (the latter would otherwise be assumed to constitute the dominant effect).

In view of this situation, the pressing question arises whether or not one should include $\delta^2 B_{60}(nS)$ into the definition of the two-loop Bethe logarithm for states with higher angular momenta. One might argue that $\delta^2 B_{60}(nS)$ should be excluded from the definition of the two-loop Bethe logarithm b_L because, as shown in Ref. [2], the term cannot be uniquely interpreted as an energy shift associated with a specific atomic level. On the other hand, one might argue that $\delta^2 B_{60}(nS)$ should be included into the definition of the two-loop Bethe logarithm b_L for higher excited states, because it is generated by the product of two imaginary energy shifts, both of which originate from the same nonrelativistic two-loop self-energy (9), which otherwise gives rise to the low-energy contribution to the B_{60} coefficient. We reemphasize that the $\delta^2 B_{60}$-term has an unambiguously defined sign for each individual state and is important for the comparison of our analytic approach to B_{60} to any nonperturbative (in $Z\alpha$) numerical calculation of the two-loop energy shift for the listed excited hydrogenic states, as well as for the comparison of theory and experiment based on a line-shape formalism [4]. Nonperturbative calculations of the two-loop self-energy have recently been pursued intensively [19–25].

In the current investigation, we would like to follow the second route and define [see Eq. (8)] $b_L = \overline{b}_L + \delta^2 B_{60}$, where $\overline{b}_L$ is obtained by performing all integrations in Eq. (10) via a principal-value prescription, with the results listed in Table II, and $\delta^2 B_{60}$ contains all the terms generated by the products of imaginary parts incurred at poles in the (k_1, k_2)-plane. This definition has the following advantages: *(i)* When the definition (8) is adopted, the term b_L in the result for the B_{60} coefficient as given in Eq. (8.1) of Ref. [6] contains all real (rather than imaginary) terms which can be inferred from the nonrelativistic self-energy given in Eq. (16) of Ref. [8] and Eq. (5) of Ref. [9] upon contour integration over both photon energies. *(ii)* In nonperturbative numerical evaluations of radiative two-loop energy shifts for excited states, one would "pick up" terms of the type $\delta^2 B_{60}$ naturally if one deforms both photon energy integration contours according to the Feynman prescription near adjacent bound-state poles. The definition (8) makes possible a direct comparison of nonperturbative numerical results obtained in this way, to the results for b_L and B_{60} given here, without the need for any subtraction of the squared imaginary parts. *(iii)* For D states, the definition (8) includes the numerically most significant real (rather than imaginary) contribution which can be inferred from the nonrelativistic two-loop self-energy (9) into b_L and thus into the B_{60} coefficient.

Despite these advantages of the proposed definition (8), one should remember that the term $\delta^2 B_{60}$ cannot be interpreted as an energy shift uniquely associated with a particular atomic level, and has to be treated differently, namely according to ideas outlined in Sec. 3 of Ref. [2] when in a comparison to experiments. According to the discussion in the cited reference, a valid way of treating (part of) $\delta^2 B_{60}$ would first entail a subtraction of this term from from the energy shift, and then, a reinterpretation of it in terms of an off-diagonal "decay rate operator" which has to be included into a line-shape formalism.

TABLE II: Numerical values for the principal-value integrated contribution $\overline{b}_L$ to the two-loop Bethe logarithms for P, D and F states. Values for S states are taken from [3] and are listed for completeness. For the $6H$ state, the result for $\overline{b}_L$ reads $-0.000(1)$, implying a negative sign.

level	$\overline{b}_L$	level	$\overline{b}_L$	level	$\overline{b}_L$	level	$\overline{b}_L$	level	$\overline{b}_L$	level	$\overline{b}_L$
$1S$	$-81.4(3)$	–	–	–	–	–	–	–	–	–	–
$2S$	$-66.6(3)$	$2P$	$-2.2(3)$	–	–	–	–	–	–	–	–
$3S$	$-63.5(6)$	$3P$	$-2.5(3)$	$3D$	$-0.006(2)$	–	–	–	–	–	–
$4S$	$-61.8(8)$	$4P$	$-2.8(3)$	$4D$	$-0.004(2)$	$4F$	$-0.002(1)$	–	–	–	–
$5S$	$-60.6(8)$	$5P$	$-2.8(3)$	$5D$	$-0.005(3)$	$5F$	$-0.002(1)$	$5G$	$-0.001(1)$	–	–
$6S$	$-59.8(8)$	$6P$	$-2.9(3)$	$6D$	$-0.006(4)$	$5F$	$-0.002(1)$	$6G$	$-0.001(1)$	$6H$	$-0.000(1)$

TABLE III: Numerical values for the correction $\delta^2 B_{60}$ for S, P, D and F states. Values for $3S$ and $4S$ have already been discussed in Ref. [3]. As explained in the text, the contributions listed below cannot be unambiguously interpreted as energy shifts associated with a particular atomic level, although they are mathematically well defined.

level	$\delta^2 B_{60}$	level	$\delta^2 B_{60}$	level	$\delta^2 B_{60}$	level	$\delta^2 B_{60}$	level	$\delta^2 B_{60}$	level	$\delta^2 B_{60}$
$1S$	0.0	–	–	–	–	–	–	–	–	–	–
$2S$	0.0	$2P$	-0.008	–	–	–	–	–	–	–	–
$3S$	-0.071	$3P$	-0.177	$3D$	0.130	–	–	–	–	–	–
$4S$	-0.109	$4P$	-0.243	$4D$	0.183	$4F$	0.027	–	–	–	–
$5S$	-0.129	$5P$	-0.276	$5D$	0.203	$5F$	0.036	$5G$	0.009	–	–
$6S$	-0.141	$6P$	-0.295	$6D$	0.215	$6F$	0.044	$6G$	0.014	$6H$	0.004

VI. EVALUATION OF B_{60}

Before we give the general result for B_{60} of P states, we would like to recall the known results for the other coefficients in Eq. (2). Specifically, we have for the spin-independent double-logarithmic term, $B_{62}(nP) = \frac{4}{27}\frac{n^2-1}{n^2}$ (see Refs. [26, 27]). Furthermore, the logarithmic terms [6] are $B_{61}(nP_{1/2}) = \frac{4}{3}\,N(nP) + \frac{n^2-1}{n^2}\left(\frac{166}{405} - \frac{8}{27}\,\ln 2\right)$ and $B_{61}(nP_{3/2}) = \frac{4}{3}\,N(nP) + \frac{n^2-1}{n^2}\left(\frac{31}{405} - \frac{8}{27}\,\ln 2\right)$. Numerical values for $N(nP)$ can be found in Eq. (17) of Ref. [28]. Based on Eq. (8.1) of Ref. [6] and on the results for b_L obtained in this paper as well as standard analytic techniques for the evaluation of matrix elements, we are now in the position to give complete results for the B_{60} coefficients of P states (see also Table IV),

$$\begin{aligned} B_{60}(nP_{1/2}) &= -\frac{27517}{25920} - \frac{209}{288\,n} + \frac{1223}{960\,n^2} + \frac{4}{27}\frac{n^2-1}{n^2}\,\ln^2(2) - \frac{38}{81}\frac{n^2-1}{n^2}\,\ln(2) \\ &+ \left(\frac{25}{6} + \frac{3}{2\,n} - \frac{9}{2\,n^2}\right)\zeta(2)\ln(2) + \left(-\frac{9151}{10800} - \frac{1}{4\,n} + \frac{1009}{1200\,n^2}\right)\zeta(2) + \left(-\frac{25}{24} - \frac{3}{8\,n} + \frac{9}{8\,n^2}\right)\zeta(3) \\ &+ \beta_4(nP_{1/2}) + \beta_5(nP_{1/2}) + \left[\frac{38}{45} - \frac{4}{3}\,\ln(2)\right]\,N(nP) + b_L(nP)\,, \end{aligned} \tag{22a}$$

$$\begin{aligned} B_{60}(nP_{3/2}) &= -\frac{73321}{103680} + \frac{185}{1152\,n} + \frac{8111}{25920\,n^2} + \frac{4}{27}\frac{n^2-1}{n^2}\,\ln^2(2) - \frac{11}{81}\frac{n^2-1}{n^2}\,\ln(2) \\ &+ \left(\frac{299}{80} - \frac{3}{8\,n} - \frac{53}{20\,n^2}\right)\zeta(2)\ln(2) + \left(-\frac{24377}{21600} + \frac{1}{16\,n} - \frac{3187}{3600\,n^2}\right)\zeta(2) + \left(-\frac{299}{320} + \frac{3}{32\,n} + \frac{53}{80\,n^2}\right)\zeta(3) \\ &+ \beta_4(nP_{3/2}) + \beta_5(nP_{3/2}) + \left[\frac{38}{45} - \frac{4}{3}\,\ln(2)\right]\,N(nP) + b_L(nP)\,. \end{aligned} \tag{22b}$$

We see that the total value of B_{60} is the sum of high-energy operators given by inverse powers of the principal quantum number, linear combinations of terms proportional to $\ln(2)$ and ζ functions of various arguments, and low-energy terms β_4 and β_5 which are known from one-loop calculations [28, 29] (see also Tables VII and VIII below), as well as the two-loop Bethe logarithm $\overline{b}_L$.

For D states, it is known that $B_{62}(nD) = B_{61}(nD) = 0$. Indeed, the fact that $N(nD) = 0$ for D states implies that the term of order $1/k_1$ in the asymptotics (15) vanishes, and this is consistent with the zero result for $B_{61}(nD)$. The nonlogarithmic

terms read [note in particular $N(nD) = 0$],

$$B_{60}(nD_{3/2}) = -\frac{125863}{2016000} - \frac{1021}{9600\,n} + \frac{18811}{60480\,n^2} + \left(\frac{1387}{8400} + \frac{9}{40\,n} - \frac{313}{420\,n^2}\right)\,\zeta(2)\ln(2) \tag{23a}$$
$$+\left(-\frac{5501}{151200} - \frac{3}{80\,n} + \frac{1073}{7560\,n^2}\right)\,\zeta(2) + \left(-\frac{1387}{33600} - \frac{9}{160\,n} + \frac{313}{1680\,n^2}\right)\,\zeta(3) + \beta_4(nD_{3/2}) + \beta_5(nD_{3/2}) + b_L(nD)\,,$$

$$B_{60}(nD_{5/2}) = \frac{61133}{6804000} + \frac{949}{21600\,n} - \frac{4967}{30240\,n^2} + \left(\frac{43}{3150} - \frac{1}{10\,n} + \frac{61}{210\,n^2}\right)\,\zeta(2)\ln(2) \tag{23b}$$
$$+\left(-\frac{421}{37800} + \frac{1}{60\,n} - \frac{29}{945\,n^2}\right)\,\zeta(2) + \left(-\frac{43}{12600} + \frac{1}{40\,n} - \frac{61}{840\,n^2}\right)\,\zeta(3) + \beta_4(nD_{5/2}) + \beta_5(nD_{5/2}) + b_L(nD)\,.$$

TABLE IV: Values of the total B_{60} coefficient for P states, derived from Eq. (22). For the numerical values of β_4 and β_5, see Tables VIII and IX in Appendix A.

level	B_{60}	level	B_{60}
$2P_{1/2}$	$-1.6(3)$	$2P_{3/2}$	$-1.8(3)$
$3P_{1/2}$	$-2.0(3)$	$3P_{3/2}$	$-2.2(3)$
$4P_{1/2}$	$-2.4(3)$	$4P_{3/2}$	$-2.5(3)$
$5P_{1/2}$	$-2.4(3)$	$5P_{3/2}$	$-2.5(3)$
$6P_{1/2}$	$-2.5(3)$	$6P_{3/2}$	$-2.6(3)$

TABLE V: Same as Table IV, but for D states. The numerical values of β_4 and β_5, which are needed for the numerical evaluation of the expressions in Eq. (23), are recorded in Tables IX and X in Appendix B.

level	B_{60}	level	B_{60}
$3D_{3/2}$	0.141(2)	$3D_{5/2}$	0.123(2)
$4D_{3/2}$	0.199(2)	$4D_{5/2}$	0.178(2)
$5D_{3/2}$	0.219(3)	$5D_{5/2}$	0.196(3)
$6D_{3/2}$	0.230(4)	$6D_{5/2}$	0.207(4)

For F states, the values of B_{60} are displayed in Table VI (detailed formulas are given in Appendix C). We observe that the total value of B_{60} for F states is numerically rather close to the value of $\delta^2 B_{60}$ for each state as given in Table II. Contributions from the fine-structure dependent terms as well as those from the high-energy operators gradually vanish as the angular momentum increases, and the dominant remaining contribution then stems from $\delta^2 B_{60}$.

For G and H states, the total value of B_{60} is the same as the value of $\delta^2 B_{60}$ up to the level of $\pm 1.0 \times 10^{-3}$ in units of B_{60}, as shown in Tables III and VI. We may now use our experience regarding the asymptotic behavior of one-loop Bethe logarithms [18] and of relativistic Bethe logarithms [29], and based on the data in Tables IV, V and Table VI for an extrapolation of B_{60} to an arbitrary state. Specifically, we conjecture that for a given hydrogenic energy level which reads nL_j in the usual spectroscopic notation,

$$B_{60}(nL_j) \approx \delta^2 B_{60} \approx \frac{1}{L^3}\,\left(1.7 - \frac{2.0}{n - L + 1}\right) \pm 50\,\%\,,$$
$$\text{for } L \geq 3, \text{ and both } j = L \pm 1/2\,. \tag{24}$$

This conjecture implies that the dominant contribution to B_{60} comes from the squared decay rates, i.e. from the term $\delta^2 B_{60}$, and the conjecture (24) can be used to estimate this coefficient for an arbitrary Rydberg state of high angular momentum.

TABLE VI: Same as Tables IV and V, but for F, G and H states. For these states, the total values of B_{60} are close to the numerical values for $\delta^2 B_{60}$ as listed in Table III, and the high-energy operators as well as the fine-structure dependent corrections do not introduce any significant numerical deviation of the total value of B_{60} from $\delta^2 B_{60}$.

level	B_{60}	level	B_{60}
$4F_{5/2}$	0.027(1)	$4F_{7/2}$	0.023(1)
$5F_{5/2}$	0.037(1)	$5F_{7/2}$	0.033(1)
$6F_{5/2}$	0.046(1)	$6F_{7/2}$	0.041(1)
$5G_{7/2}$	0.009(1)	$5G_{9/2}$	0.008(1)
$6G_{7/2}$	0.014(1)	$6G_{9/2}$	0.013(1)
$6H_{9/2}$	0.004(1)	$6H_{11/2}$	0.004(1)

VII. CONCLUSIONS

Together with the one-loop results from Appendix D, the reported calculation of the two-loop nonlogarithmic term of order $(\alpha/\pi)^2\,(Z\alpha)^2\,m_{\rm e}\,c^2$ completes the analysis of the quantum electrodynamic corrections to non-S states in the order $\alpha^8\,m_{\rm e}\,c^2$ for hydrogen ($Z = 1$). Together with other recent theoretical investigations [6, 7], the current work clarifies further prerequisites and the theoretical basis for the determination of fundamental constants from hydrogen spectroscopy at the level of one part in 10^{14}. For ionized helium, the corrections calculated here are enhanced by a factor of $2^6 = 64$ in frequency units. The numerical values of principal-value two-loop Bethe logarithms $\overline{b}_L$ are given in Table II, and squared decay rates $\delta^2 B_{60}$ are indicated in Table III. Final numerical results for B_{60}, which is the sum of $\overline{b}_L$, $\delta^2 B_{60}$ and high-

energy operators as well as fine-structure dependent terms [see Eqs. (22a)—(23b)], are given in Tables IV, V and VI. Our total results for B_{60} contain the sum of the contributions from all four gauge-invariant subsets as shown in Fig. 2. We confirm that the trend already observed in the literature [17, 18] for one-loop Bethe logarithms which decrease in magnitude with increasing orbital angular momentum quantum number, also holds for the two-loop counterparts. Finally, a comparison of our results with a very recent numerical investigation [25] indicates that our results for $B_{60}(2P_{1/2})$ and $B_{60}(2P_{3/2})$ for subset i (see Fig. 2 and Tables VII and VIII below) are consistent with a nonperturbative (in $Z\alpha$) treatment of the two-loop self-energy, which forms subset i in the classification of Fig. 2.

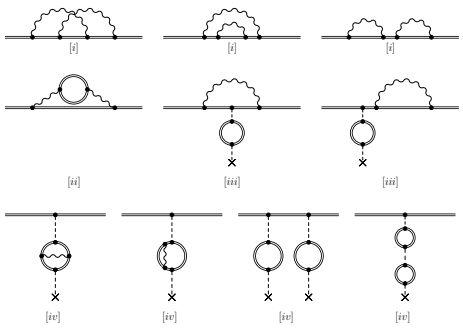

FIG. 2: The two-loop diagrams which give rise to the B_{60} coefficient naturally fall into four gauge-invariant subsets, labeled i–iv (we follow the classification of diagrams according to Ref. [6]). Our results for B_{60} contain contributions from all of these diagrams; the separation into the four subsets is only relevant for the detailed formulas given in the Appendixes.

The connection of the two-loop problem to squared decay rates has been analyzed previously in Refs. [2, 3]. For the atomic levels under investigation, we give a respective treatment in Sec. V. The contributions to B_{60} in Table III due to squared imaginary parts cannot be interpreted as energy shifts in the usual sense and set a limit to the actual "definability" of the atomic energy levels under investigation. The surprising conclusion of the current investigation is that the squared decay rates actually give the dominant contribution to B_{60} for states with higher angular momenta (see Tables II, III and VI). As $\delta^2 B_{60}$ cannot be associated uniquely as an energy correction to one specific atomic level, we conclude that our calculation explores the predictive limits of quantum electrodynamic theory of energy levels of the hydrogen atom and hydrogenlike systems. Explicit theoretical values of the Lamb shift for selected states in hydrogenlike ions will be presented elsewhere.

All calculations reported here (see in particular Tables II and III) were carried out on an average-size cluster of workstations. A fifth-order finite-difference scheme was used in order to accurately describe the behavior of the S component of the propagators on a grid near the origin, and in order to allow for a fast calculation of the two-loop integrand on the workstation cluster of Max–Planck–Institute for Nuclear Physics in Heidelberg and of the National Institute of Standards and Technology. However, even the most sophisticated computer hardware and numerical algorithms would be useless in the current context unless combined with a thorough formulation of the subtraction procedures necessary to extract the physically observable energy corrections and frequency shifts.

Acknowledgments

The author acknowledges support from the Deutsche Forschungsgemeinschaft (Heisenberg program). Helpful conversations with Krzysztof Pachucki, Vladimir A. Yerokhin and Peter J. Mohr are gratefully acknowledged. The stimulating atmosphere at the National Institute of Standards and Technology has contributed to the completion of this project.

APPENDIX A: MISCELLANEOUS RESULTS FOR P STATES

In Sec. VI, we had discussed the evaluation of the total B_{60} coefficient for $P_{1/2}$ and $P_{3/2}$ states of general n. Here, we would like to supplement the results for the individual subsets i–iv of the two-loop diagrams as given in Figs. 1–4 of Ref. [6] and in Fig. 2 here. The results presented in this Appendix might be helpful both for a comparison of our analytic to nonperturbative numerical results, as well as for a verification of alternative, independent analytic calculations for particular sets of diagrams.

We start with the subset i (pure two-loop self-energy) for $P_{1/2}$ states (see Fig. 2),

$$B^i_{60}(nP_{1/2}) = \frac{3829}{77760} + \frac{89}{96\,n} - \frac{44437}{77760\,n^2} + \frac{4}{27}\,\frac{n^2-1}{n^2}\,\ln^2(2) - \frac{38}{81}\,\frac{n^2-1}{n^2}\,\ln(2)$$
$$+ \left(\frac{25}{6} + \frac{3}{2\,n} - \frac{9}{2\,n^2}\right)\,\zeta(2)\ln(2) + \left(-\frac{7613}{5400} - \frac{5}{4\,n} + \frac{1663}{900\,n^2}\right)\,\zeta(2) + \left(-\frac{25}{24} - \frac{3}{8\,n} + \frac{9}{8\,n^2}\right)\,\zeta(3)$$
$$+ \beta_4(nP_{1/2}) + \beta_5(nP_{1/2}) + \left[\frac{10}{9} - \frac{4}{3}\,\ln(2)\right]\,N(nP) + b_L(nP)\,. \qquad \text{(A1)}$$

TABLE VII: Breakdown of the individual contributions to $B_{60}(nP_{1/2})$ from all diagrammatic subsets as defined in Ref. [6]. The numerical uncertainty in $B^i_{60}(nP_{1/2})$ is entirely due to the two-loop Bethe logarithm given in Table II. The N term has been calculated in Ref. [28]; it is spin-independent and therefore indicated only for the $P_{1/2}$ states (cf. Table VIII below).

level	β_4	β_5	N	B^i_{60}	B^{ii}_{60}	B^{iii}_{60}	B^{iv}_{60}
$2P_{1/2}$	-0.314 100	0.260 017	0.003 301	-1.5(3)	0.017 642	-0.034 214	-0.126 543
$3P_{1/2}$	-0.362 439	0.292 936	0.003 572	-1.8(3)	0.022 297	-0.040 459	-0.149 977
$4P_{1/2}$	-0.380 983	0.304 244	-0.000 394	-2.2(3)	0.024 123	-0.041 562	-0.158 179
$5P_{1/2}$	-0.390 543	0.309 438	-0.004 304	-2.2(3)	0.025 057	-0.041 519	-0.161 975
$6P_{1/2}$	-0.396 287	0.312 249	-0.007 497	-2.3(3)	0.025 613	-0.041 211	-0.164 037

We also note that in Eqs. (5.4), (6.2) and (7.7) of Ref. [6], results for the fine-structure difference associated with the diagrams of subsets ii–iv were indicated. We reemphasize that these results are valid only for the fine-structure difference of P states. Therefore, we would like to supplement the individual contributions for $P_{1/2}$ and $P_{3/2}$ here, starting with $P_{1/2}$,

$$B^{ii}_{60}(nP_{1/2}) = -\frac{1939}{2160} - \frac{119}{72\,n} + \frac{10577}{6480\,n^2} + \left(\frac{9}{16} + \frac{1}{n} - \frac{145}{144\,n^2}\right)\,\zeta(2)\,, \tag{A2}$$

$$B^{iii}_{60}(nP_{1/2}) = -\frac{2}{45}\,\left(1 - \frac{1}{n^2}\right) - \frac{4}{15}\,N(nP)\,, \qquad B^{iv}_{60}(nP_{1/2}) = -\frac{41}{243}\,\left(1 - \frac{1}{n^2}\right)\,. \tag{A3}$$

For the two-loop self-energy subset i, we obtain in the case of a $P_{3/2}$ state,

$$\begin{aligned} B^{i}_{60}(nP_{3/2}) &= -\frac{73321}{103680} + \frac{185}{1152\,n} + \frac{8111}{25920\,n^2} + \frac{4}{27}\frac{n^2-1}{n^2}\,\ln^2(2) - \frac{11}{81}\frac{n^2-1}{n^2}\,\ln(2) \\ &+ \left(\frac{299}{80} - \frac{3}{8\,n} - \frac{53}{20\,n^2}\right)\,\zeta(2)\ln(2) + \left(-\frac{24377}{21600} + \frac{1}{16\,n} - \frac{3187}{3600\,n^2}\right)\,\zeta(2) + \left(-\frac{299}{320} + \frac{3}{32\,n} + \frac{53}{80\,n^2}\right)\,\zeta(3) \\ &+ \beta_4(nP_{3/2}) + \beta_5(nP_{3/2}) + \left[\frac{10}{9} - \frac{4}{3}\,\ln(2)\right]\,N(nP) + b_L(nP)\,. \end{aligned} \tag{A4}$$

The contributions of the diagrammatic subsets ii–iv read as follows,

$$B^{ii}_{60}(nP_{3/2}) = -\frac{3595}{5184} + \frac{119}{288\,n} - \frac{11}{88\,n^2} + \left(\frac{17}{40} - \frac{1}{4\,n} + \frac{7}{90\,n^2}\right)\,\zeta(2) \tag{A5}$$

$$B^{iii}_{60}(nP_{3/2}) = -\frac{1}{45}\,\left(1 - \frac{1}{n^2}\right) - \frac{4}{15}\,N(nP)\,, \qquad B^{iv}_{60}(nP_{3/2}) = -\frac{41}{486}\,\left(1 - \frac{1}{n^2}\right)\,. \tag{A6}$$

It is perhaps also instructive to indicate here, the total result for the fine-structure difference of B_{60}. In Ref. [6], only the individual subsets i–iv were treated for the fine-structure, but their sum was not indicated, and this "checksum" is supplemented here:

$$\begin{aligned} B_{60}(nP_{3/2}) - B_{60}(nP_{1/2}) &= \frac{1361}{3840} + \frac{1021}{1152\,n} - \frac{2491}{2592\,n^2} + \frac{1}{3}\frac{n^2-1}{n^2}\,\ln(2) + \left(-\frac{103}{240} - \frac{15}{8\,n} + \frac{37}{20\,n^2}\right)\,\zeta(2)\ln(2) \\ &+ \left(-\frac{9}{32} + \frac{5}{16\,n} + \frac{2}{45\,n^2}\right)\,\zeta(2) + \left(\frac{103}{960} + \frac{15}{32\,n} - \frac{37}{80\,n^2}\right)\,\zeta(3) + \beta_4(nP_{3/2}) - \beta_4(nP_{1/2}) + \beta_5(nP_{3/2}) - \beta_5(nP_{1/2})\,. \end{aligned} \tag{A7}$$

In this result, b_L cancels, and $B_{60}(nP_{3/2}) - B_{60}(nP_{1/2})$ evaluates, e.g., to a numerical value of -0.134817 for $n = 2$. The reader may consult Tables VII and VIII for details and observe that the principal numerical uncertainty due to b_L cancels for the fine-structure.

TABLE VIII: Same as Table VII, but for $nP_{3/2}$.

level	β_4	β_5	B_{60}^{i}	B_{60}^{ii}	B_{60}^{iii}	B_{60}^{iv}
$2P_{3/2}$	0.157 050	-0.130 009	-1.8(3)	0.004 207	0.015 786	0.063 272
$3P_{3/2}$	0.181 219	-0.146 468	-2.2(3)	0.005 208	0.018 801	0.074 989
$4P_{3/2}$	0.190 492	-0.152 122	-2.6(3)	0.005 510	0.020 938	0.079 090
$5P_{3/2}$	0.195 271	-0.154 719	-2.6(3)	0.005 627	0.022 481	0.080 988
$6P_{3/2}$	0.198 144	-0.156 124	-2.7(3)	0.005 678	0.023 604	0.082 019

APPENDIX B: MISCELLANEOUS RESULTS FOR D STATES

For D states, we observe that only subsets i and ii contribute and start with $D_{3/2}$,

$$B_{60}^{i}(nD_{3/2}) = \frac{405431}{6048000} + \frac{453}{3200\,n} - \frac{4901}{12096\,n^2} + \left(\frac{1387}{8400} + \frac{9}{40\,n} - \frac{313}{420\,n^2}\right)\zeta(2)\ln(2)$$
$$+ \left(-\frac{3469}{30240} - \frac{3}{16\,n} + \frac{4349}{7560\,n^2}\right)\zeta(2) + \left(-\frac{1387}{33600} - \frac{9}{160\,n} + \frac{313}{1680\,n^2}\right)\zeta(3)$$
$$+ \beta_4(nD_{3/2}) + \beta_5(nD_{3/2}) + b_L(nD)\,. \tag{B1}$$

Subset ii yields,

$$B_{60}^{ii}(nD_{3/2}) = -\frac{5593}{43200} - \frac{119}{480\,n} + \frac{1547}{2160\,n^2} + \left(\frac{47}{600} + \frac{3}{20\,n} - \frac{13}{30\,n^2}\right)\zeta(2)\,. \tag{B2}$$

We now continue with $D_{5/2}$,

$$B_{60}^{i}(nD_{5/2}) = -\frac{21503}{756000} - \frac{53}{800\,n} + \frac{1577}{6048\,n^2} + \left(\frac{43}{3150} - \frac{1}{10\,n} + \frac{61}{210\,n^2}\right)\zeta(2)\ln(2)$$
$$+ \left(\frac{39}{2520} + \frac{1}{12\,n} - \frac{272}{945\,n^2}\right)\zeta(2) + \left(-\frac{43}{12600} + \frac{1}{40\,n} - \frac{61}{840\,n^2}\right)\zeta(3) + \beta_4(nD_{5/2}) + \beta_5(nD_{5/2}) + b_L(nP)\,. \tag{B3}$$

Here, subset ii yields

$$B_{60}^{ii}(nD_{5/2}) = \frac{1819}{48600} + \frac{119}{1080\,n} - \frac{17}{40\,n^2} + \left(-\frac{107}{4725} - \frac{1}{15\,n} + \frac{9}{35\,n^2}\right)\zeta(2)\,. \tag{B4}$$

Subsets iii and iv do not contribute in either case for D states. A "checksum" for the total fine-structure difference can be useful,

$$B_{60}(nD_{5/2}) - B_{60}(nD_{3/2}) = \frac{777473}{10886400} + \frac{2597}{17280\,n} - \frac{5749}{12096\,n^2} + \left(-\frac{3817}{25200} - \frac{13}{40\,n} + \frac{29}{28\,n^2}\right)\zeta(2)\ln(2)$$
$$+ \left(\frac{3817}{151200} + \frac{13}{240\,n} - \frac{29}{168\,n^2}\right)\zeta(2) + \left(\frac{3817}{100800} + \frac{13}{160\,n} - \frac{29}{112\,n^2}\right)\zeta(3)$$
$$+ \beta_4(nD_{5/2}) - \beta_4(nD_{3/2}) + \beta_5(nD_{5/2}) - \beta_5(nD_{3/2})\,. \tag{B5}$$

In this result, b_L cancels, and the quantity $B_{60}(nD_{5/2}) - B_{60}(nD_{3/2})$ evaluates, e.g., to a numerical value of -0.018197 for $n = 2$. The interested reader may consult Tables IX and X for details, observing that the principal numerical uncertainty due to b_L cancels for the fine-structure.

TABLE IX: Breakdown of the individual contributions to $B_{60}(nD_{3/2})$ from all diagrammatic subsets as defined in Ref. [6]. The numerical uncertainty in $B^i_{60}(nD_{3/2})$ is entirely due to the two-loop Bethe logarithm given in Table II.

level	β_4	β_5	B^i_{60}	B^{ii}_{60}
$3D_{3/2}$	-0.002 361	0.005 397	0.141(2)	-0.000 629
$4D_{3/2}$	-0.002 883	0.006 280	0.199(2)	-0.000 696
$5D_{3/2}$	-0.003 101	0.006 675	0.220(3)	-0.000 714
$6D_{3/2}$	-0.003 200	0.006 886	0.230(4)	-0.000 716

TABLE X: Same as Table IX, but for $nD_{5/2}$.

level	β_4	β_5	B^i_{60}	B^{ii}_{60}
$3D_{5/2}$	0.001 574	-0.003 598	0.123(2)	0.000 128
$4D_{5/2}$	0.001 922	-0.004 186	0.177(2)	0.000 182
$5D_{5/2}$	0.002 067	-0.004 450	0.196(3)	0.000 202
$6D_{5/2}$	0.002 133	-0.004 591	0.207(4)	0.000 209

APPENDIX C: MISCELLANEOUS RESULTS FOR F, G AND H STATES

For states with angular momenta $l = 3, 4, 5$, we indicate here only the final results for B_{60}, without considering the breakdown for the terms generated by the individual subsets in Fig. 2. We obtain for $F_{5/2}$ states,

$$\begin{aligned} B_{60}(nF_{5/2}) = & -\frac{8321}{666792} - \frac{1415}{42336\,n} + \frac{2567}{18144\,n^2} + \left(\frac{71}{2205} + \frac{1}{14\,n} - \frac{209}{630\,n^2}\right)\zeta(2)\ln(2) \\ & + \left(-\frac{2173}{317520} - \frac{1}{84\,n} + \frac{347}{5670\,n^2}\right)\zeta(2) + \left(-\frac{71}{8820} - \frac{1}{56\,n} + \frac{209}{2520\,n^2}\right)\zeta(3) \\ & + \beta_4(nF_{5/2}) + \beta_5(nF_{5/2}) + b_L(nF)\,. \end{aligned} \tag{C1}$$

For $F_{7/2}$ states, the result reads

$$\begin{aligned} B_{60}(nF_{7/2}) = & \frac{994501}{284497920} + \frac{1343}{75264\,n} - \frac{33031}{362880\,n^2} + \left(-\frac{125}{56448} - \frac{9}{224\,n} + \frac{89}{504\,n^2}\right)\zeta(2)\ln(2) \\ & + \left(-\frac{5629}{5080320} + \frac{3}{448\,n} - \frac{1067}{45360\,n^2}\right)\zeta(2) + \left(\frac{125}{225792} + \frac{9}{896\,n} - \frac{89}{2016\,n^2}\right)\zeta(3) \\ & + \beta_4(nF_{7/2}) + \beta_5(nF_{7/2}) + b_L(nF)\,. \end{aligned} \tag{C2}$$

$G_{7/2}$ states provide us with the following information,

$$\begin{aligned} B_{60}(nG_{7/2}) = & -\frac{762011}{191600640} - \frac{67}{4608\,n} + \frac{2389}{29568\,n^2} + \left(\frac{2677}{266112} + \frac{1}{32\,n} - \frac{1037}{5544\,n^2}\right)\zeta(2)\ln(2) \\ & + \left(-\frac{16601}{7983360} - \frac{1}{192\,n} + \frac{3379}{99792\,n^2}\right)\zeta(2) + \left(-\frac{2677}{1064448} - \frac{1}{128\,n} + \frac{1037}{22176\,n^2}\right)\zeta(3) \\ & + \beta_4(nG_{7/2}) + \beta_5(nG_{7/2}) + b_L(nG)\,, \end{aligned} \tag{C3}$$

whereas $G_{9/2}$ states yield

$$B_{60}(nG_{9/2}) = \frac{170587}{112266000} + \frac{193}{21600\,n} - \frac{1277}{22176\,n^2} + \left(-\frac{44}{23625} - \frac{1}{50\,n} + \frac{73}{630\,n^2}\right)\zeta(2)\ln(2)$$
$$+ \left(-\frac{1153}{12474000} + \frac{1}{300\,n} - \frac{1037}{62370\,n^2}\right)\zeta(2) + \left(\frac{11}{23625} + \frac{1}{200\,n} - \frac{73}{2520\,n^2}\right)\zeta(3)$$
$$+ \beta_4(nG_{9/2}) + \beta_5(nG_{9/2}) + b_L(nG)\,. \tag{C4}$$

The results for $H_{9/2}$

$$B_{60}(nH_{9/2}) = -\frac{9169711}{5606172000} - \frac{2203}{290400\,n} + \frac{19361}{370656\,n^2} + \left(\frac{14411}{3539250} + \frac{9}{550\,n} - \frac{1543}{12870\,n^2}\right)\zeta(2)\ln(2)$$
$$+ \left(-\frac{104891}{127413000} - \frac{3}{1100\,n} + \frac{1241}{57915\,n^2}\right)\zeta(2) + \left(-\frac{14411}{14157000} - \frac{9}{2200\,n} + \frac{1543}{51480\,n^2}\right)\zeta(3)$$
$$+ \beta_4(nH_{9/2}) + \beta_5(nH_{9/2}) + b_L(nH)\,, \tag{C5}$$

and $H_{11/2}$

$$B_{60}(nH_{11/2}) = \frac{4047937}{5381925120} + \frac{2131}{418176\,n} - \frac{29401}{741312\,n^2} + \left(-\frac{85}{75504} - \frac{1}{88\,n} + \frac{419}{5148\,n^2}\right)\zeta(2)\ln(2)$$
$$+ \left(\frac{877}{20386080} + \frac{1}{528\,n} - \frac{1123}{92664\,n^2}\right)\zeta(2) + \left(\frac{85}{302016} + \frac{1}{352\,n} - \frac{419}{20592\,n^2}\right)\zeta(3)$$
$$+ \beta_4(nH_{11/2}) + \beta_5(nH_{11/2}) + b_L(nH) \tag{C6}$$

complete the investigation of B_{60} coefficients.

APPENDIX D: VACUUM POLARIZATION AND SELF ENERGY SHIFTS OF ORDER $\alpha\,(Z\alpha)^7$

As is well known, the one-loop (1L) vacuum polarization (VP) correction scales as

$$\Delta E^{(1\mathrm{L})}_{\mathrm{VP}} = \frac{\alpha}{\pi}\,\frac{(Z\alpha)^4}{n^3}\,F_{\mathrm{VP}}(Z\alpha)\,, \tag{D1}$$

where $F_{\mathrm{VP}}(Z\alpha)$ is a dimensionless function. The first few terms of $F_{\mathrm{VP}}(Z\alpha)$ for S states can be found in a number of review articles, e.g. [30, 31]. E.g., the lowest-order term for S states is $A^{\mathrm{VP}}_{40}(nS) = -4/15$. The first index of the A^{VP}-coefficients denotes the power of $Z\alpha$, and the second denotes the power of $\ln[(Z\alpha)^{-2}]$.

For states with nonvanishing angular momenta, it is well known that the leading terms in the expansion of $F_{\mathrm{VP}}(Z\alpha)$ vanish. In the order $\alpha(Z\alpha)^6$, the leading coefficients for P states [32] are known to read as follows,

$$A^{\mathrm{VP}}_{60}(nP_{1/2}) = -\frac{3}{35}\,\frac{n^2-1}{n^2}\,, \tag{D2a}$$

$$A^{\mathrm{VP}}_{60}(nP_{3/2}) = -\frac{2}{105}\,\frac{n^2-1}{n^2}\,. \tag{D2b}$$

An investigation of the behavior of the wave functions near the nucleus, inspired by Ref. [33], leads to the following correction terms of order $\alpha(Z\alpha)^7$,

$$A^{\mathrm{VP}}_{70}(nP_{1/2}) = \frac{41\pi}{2304}\,\frac{n^2-1}{n^2}\,, \tag{D3a}$$

$$A^{\mathrm{VP}}_{70}(nP_{3/2}) = \frac{7\pi}{768}\,\frac{n^2-1}{n^2}\,. \tag{D3b}$$

These results are consistent with the particular case $n = 2$ treated on p. 124 of Ref. [31], for which the coefficients read $A_{70}(2P_{1/2}) = 41\pi/3072$ and $A_{70}(2P_{3/2}) = 7\pi/1024$. Both the A^{VP}_{60} as well as the A^{VP}_{70} coefficients vanish for D states and all states with higher angular momenta. Note that the self-energy remainder function G_{SE}, as calculated in Refs. [34, 35] for P states, contains all contributions of order $\alpha\,(Z\alpha)^7$ due to the one-photon self-energy. For D states and states with higher angular momenta, self-energy shifts of order $\alpha\,(Z\alpha)^6$ have been compiled, e.g., in Ref. [14], and the self-energy corrections of order $\alpha\,(Z\alpha)^7$ vanish. These remarks supplement the above results for the one-loop vacuum polarization.

[1] H. A. Bethe, Phys. Rev. **72**, 339 (1947).
[2] U. D. Jentschura, J. Evers, C. H. Keitel, and K. Pachucki, New J. Phys. **4**, 49 (2002).
[3] U. D. Jentschura, Phys. Rev. A **70**, 052108 (2004).
[4] F. Low, Phys. Rev. **88**, 53 (1952).
[5] P. J. Mohr and B. N. Taylor, Rev. Mod. Phys. **77**, 1 (2005).
[6] U. D. Jentschura, A. Czarnecki, and K. Pachucki, Phys. Rev. A **72**, 062102 (2005).
[7] A. Czarnecki, U. D. Jentschura, and K. Pachucki, Phys. Rev. Lett. **95**, 180404 (2005).
[8] K. Pachucki, Phys. Rev. A **63**, 042503 (2001).
[9] K. Pachucki and U. D. Jentschura, Phys. Rev. Lett. **91**, 113005 (2003).
[10] V. B. Berestetskii, E. M. Lifshitz, and L. P. Pitaevskii, *Quantum Electrodynamics* (Pergamon Press, Oxford, UK, 1982).
[11] K. Pachucki, Ann. Phys. (N.Y.) **226**, 1 (1993).
[12] U. Jentschura and K. Pachucki, Phys. Rev. A **54**, 1853 (1996).
[13] U. D. Jentschura and K. Pachucki, J. Phys. A **35**, 1927 (2002).
[14] U. D. Jentschura, Mod. Phys. Lett. A **20**, 2261 (2005).
[15] S. Salomonson and P. Öster, Phys. Rev. A **40**, 5559 (1989).
[16] A. Poquerusse, Phys. Lett. A **82**, 232 (1981).
[17] G. W. F. Drake and R. A. Swainson, Phys. Rev. A **41**, 1243 (1990).
[18] U. D. Jentschura and P. J. Mohr, Phys. Rev. A **72**, 012110 (2005).
[19] S. Mallampalli and J. Sapirstein, Phys. Rev. A **57**, 1548 (1998).
[20] S. Mallampalli and J. Sapirstein, Phys. Rev. Lett. **80**, 5297 (1998).
[21] V. A. Yerokhin and V. M. Shabaev, Phys. Rev. A **64**, 062507 (2001).
[22] V. A. Yerokhin, P. Indelicato, and V. M. Shabaev, Phys. Rev. Lett. **91**, 073001 (2003).
[23] V. A. Yerokhin, P. Indelicato, and V. M. Shabaev, Zh. Éksp. Teor. Fiz. **128**, 322 (2005), [JETP Lett. **101**, 280 (2005)].
[24] V. A. Yerokhin, P. Indelicato, and V. M. Shabaev, Phys. Rev. A **71**, R040101 (2005).
[25] V. A. Yerokhin, P. Indelicato, and V. M. Shabaev, preprint (unpublished) and private communication (2006).
[26] S. G. Karshenboim, J. Phys. B **29**, L29 (1996).
[27] U. D. Jentschura and I. Nándori, Phys. Rev. A **66**, 022114 (2002).
[28] U. D. Jentschura, J. Phys. A **36**, L229 (2003).
[29] U. D. Jentschura, E.-O. Le Bigot, P. J. Mohr, P. Indelicato, and G. Soff, Phys. Rev. Lett. **90**, 163001 (2003).
[30] J. Sapirstein and D. R. Yennie, in *Quantum Electrodynamics*, Vol. 7 of *Advanced Series on Directions in High Energy Physics*, edited by T. Kinoshita (World Scientific, Singapore, 1990), pp. 560–672.
[31] M. I. Eides, H. Grotch, and V. A. Shelyuto, Phys. Rep. **342**, 63 (2001).
[32] U. D. Jentschura, G. Soff, and P. J. Mohr, Phys. Rev. A **56**, 1739 (1997).
[33] J. Schwinger, *Particles, Sources and Fields* (Addison-Wesley, Reading, MA, 1970).
[34] U. D. Jentschura, P. J. Mohr, and G. Soff, Phys. Rev. A **63**, 042512 (2001).
[35] U. D. Jentschura and P. J. Mohr, Phys. Rev. A **72**, 014103 (2005).